Journal of Progressive Research in Mathematics
Vol 18,4 - 2021 — E-ISSN: 2395-0218
http://www.scitecresearch.com/journals/index.php/jprm

Mathematical Modeling of Host - Pest Interactions in Stage-Structured Populations: A Case of False Codling Moth [*Thaumatotibia leucotreta*]

Jimrise O. Ochwach[1], Mark O. Okongo[1], Moses M. Muraya[2]

[a1]*Department of Physical Sciences, Chuka University, P.O. Box 109-60400, Kenya.*

[b2]*Department of Plant Sciences, Chuka University, P.O. Box 109-60400, Kenya*
Emails: ojimrise09@gmail.com; marikookongo@gmail.com; mosesmuraya@gmail.com
okongo@chuka.ac.ke, moses.muraya@chuka.ac.ke

Received: August 18, 2021; Accepted: September 11, 2021; Published: September 27, 2021

Abstract

False codling moth (FCM) (*Thaumatotibia lucotreta*) is a significant pest due to its potential economic impact on many susceptible fruits in most temperate regions of the world. Efforts to control the codling moth in the past mostly relied on the use of broad spectrum insecticide sprays, which has resulted in the development of insecticide resistance, and the disruption of the control of secondary pests. Understanding the dynamic of this pest is of great in importance in order to effectively employ the most effective control strategies. In this study, a mathematical model of host-false codling moth interactions is developed and qualitatively analysed using stability theory of system of differential equations. The basic offspring number with respect to FCM free equilibrium is obtain using next generation matrix. The condition for local and global asymptotic stability of FCM free and coexistence equilibria are established. The model is analysed numerically and graphically represented to justify the analytical results.

Keywords:

Mathematical modeling, False codling moth, stability Analysis, Host-pest interactions, Plant pest model.

1. Introduction

False codling moth (FCM), *(Thaumatotibia leucotreta)* is considered the most significant indigenous pest due to its potential economic impact on many horticultural and agricultural crops (Gillaga et al., 2011). larval attack over 70 host plants, many of which are horticultural crops with fruit, pods, and berries, such as beans, grapes, citrus, capsicum, avocado, guava, pomegranate, and ornamental plants. They also feed on macadamia nuts, cotton, tea, and a variety of other wild plants. Female moths are attracted to lay their eggs on the flower heads as well as other parts of the plant, making this pest particularly problematic on roses grown for cut flowers (Venette *et al*., 2003).

Consequently, FCM is a major threat to food security, supply of raw material for manufacturing, foreign exchange

How to cite this paper: Jimrise O. Ochwach, Mar1k O. Okongo, Moses M. Muraya (2021) Mathematical Modeling of Host - Pest Interactions in Stage-Structured Populations: A Case of False Codling Moth [*Thaumatotibia leucotreta*. Journal of Progressive Research in Mathematics, 18(4), 1-21. Retrieved from http://scitecresearch.com/journals/index.php/jprm/article/view/2087

and employment in many countries (Blomefield *et al*., 1989; Gillaga *et al*., 2011). FCM is widely distributed across Africa and has been reported in over 40 Africa countries , including Kenya (Venette *et al*., 2003; Stibick. 2008). The FCM is not considered to be established outside of Africa (Venette *et al*., 2003). However, it is commonly intercepted during quarantine inspections in Europe and United States (Gianni *et al*., 2014).

Consignments of roses from Kenya to Europe have been intercepted in recent years due to the presence of FCM. When a single living individual of FCM is found within a consignment at any stage of development, the entire consignment is rejected (FPEAK, 2021). This is because FCM is on the European Commission's (EC) list of harmful organisms that should be regulated as quarantine pests to prevent its introduction into Europe, where it could harm a variety of outdoor and greenhouse crops (Moore, 2012; Mkiga *et al*., 2019). Therefore, FCM is a pest of phytosanitary concern and it impedes export in most international markets, as it is endemic to sub-Saharan Africa (Hofmeyr *et al*., 1998; Moore, 2012).

False codling moth is now a quarantine pest on all crops according European Union (EU) plant health (phytosanitary) regulations (EU 2016/2031). Special measures have been introduced for crops that are a known pathway into the EU for serious pests that could damage Europe's agriculture or environment. These measures include stringent new requirements covering the export of roses to prevent the introduction of FCM into the EU (FPEAK, 2021). The number of FCM interceptions on Kenyan roses has been extremely high (36 in 2018, 36 in 2019, and 24 up to June 2020). This high level of interceptions has been attributed to increased inspection levels, which have risen from 5% in 2011 to 10% now. In 2021, a drastic increase to 50% or even 100% checks for roses from Kenya is expected as a result of the numbers observed in the previous three years. By the end of 2020, this will be determined (FPEAK, 2021).

Planning efficient and cost-effective FCM control is a real challenge, which explains why most experimental FCM control strategies fail (Anguelove *et al* ., 2016). This is because certain parameters can be changed to make biological systems unstable or stable, i.e., if their values pass through bifurcation values. (Murray, 2002; Sergio, 2014; Savary, 2006). Therefore, there is need for more scientific studies on FCM interaction with the host for effective management of the pest.

The demand for reliable pest infestation models is increasing because they are helpful in defining problems, organizing thoughts, identifying areas to investigate, making predictions, generating hypotheses, and supporting pest management decision-making. They also serve as standard comparisons and offer strategies to improve decision-making on effective pest control (Byers, 1993 & Anguelov *et al*., 2016). Predicting population dynamics and evaluating pest control scenarios by agro-ecosystem under a variety of environmental conditions can reduce the number and cost of pest control interventions, improving crop yields and quality, as well as health and sustainability (Galilio *et al*., 2014).

Conventional population growth models have been used and modified over time to provide an intuitive foundation for understanding the results of more complex eco-epidemiology modeling (Anderson and May, 1978; Ludwig, 1978; Anderson and May 1979). Recently, these models have been extended to explain the dynamics of human infectious diseases such Malaria, Tuberculosis (TB), Human Immunodeficiency Virus (HIV) and Acquired Immune Deficiency Syndrome (AIDS) and crop diseases (Okongo, 2016). However, very little attention have been given to host- pest interactions particularly in insect pest management. This study attempt to develop the host pest interaction model to simulate stage structure ofFCM interaction with the host.

Demographic models with stage structures have been used to describe changes in population abundance over time and across generations. Since population abundance is the major driving force acting on the host plants, this provides an opportunity to interpret the impact of pest populations on both natural and cultivated plants. (Barclay, 2016 & Galilio *et al*., 2014).

Several differential equations have been used to explain empirical data sets for single species pest population fluctuation over time, both in continuous and discrete forms. Ikemoto *et al*, (2009) developed a mathematical model for caste differentiation in termite colonies via hormonal and pheromonal regulation to aid in the discovery of primer pheromones and inferring their roles in termite caste differentiation. Barclay and Hariotakis, (1991) developed age-structured population dynamic model combining pheromone baited and food baited traps for insect pest control. Similar models of mating disruption and mass trapping were also developed by Byers, (2007). Sterile release models were developed by Anguelove *et al*, (2012) to control anopheles mosquito and Barclay (2016) to determine the rate of sterile release. However, most of these mathematical models do not address the population dynamics of FCM and its

interaction with the host which this study is seeking to address. In this study, a mathematical model of host -FCM interactions is developed and numerically analysed and results presented in graphical form.

2 Model development

In the absence of pest, the susceptible S_h host grows logistically to maturity at the rate $\alpha S_h(t)\ 1 - \frac{S_h(t)}{K}$, with α as the intrinsic growth rate and K as the environmental carrying capacity. Hosts can only be infected by the FCM after the fertilized fertile female (F_{ff}) deposit egg which successfully hatch into larvae and burrow into rind the host (Stibick, 2006). Once the host fruit is infected by the larvae (L_f) it never recovers and gives no yield (Alemneh *et al*., 2019), it can then be removed from the farm or fall on the ground. It is assumed that the host invasion follows Holling-type II functional response $\frac{\xi S_h(t) L_f(t)}{m+S_h(t)}$, where ξ is the invasion rate of the host by the larvae and m is the half saturation constant (Tazerouni *et al*., 2019). Once healthy host grows to maturity, they are harvested at the rate μ_1. Then, from the above assumptions, the equation that governs the susceptible host compartment is given by equation 1:

$$\frac{dS_h(t)}{dt} = \alpha\left(1 - \frac{S_h(t)}{K_h}\right) S_h(t) - \frac{\xi S_h(t) L_f(t)}{m + S_h(t)} - \mu_1 S_h(t) \tag{1}$$

It is important to note that the total population of FCM consists of Egg (E_f), Larvae (L_f), Pupae (P_f) and Adult(Fertile female (F_f), Fertile male (M_f) and Fertilized fertile female (F_{ff})). Each developmental stage is dependent on temperature and availability of food (Stibick *et al*., 2008).

The number of eggs produced is determined by the oviposition rate rF_{ff}, where r is the intrinsic egg laying rate and F_{ff} is the number of fertilized fertile female of FCM. Since eggs are constrained to the carrying capacity of the host, the effective egg production rate is given by $rF_{ff}\ 1 - \frac{E_f(t)}{A}\ \varphi S_h(t)$, where $1 - \frac{E_f(t)}{A}\ \varphi S_h(t)$ is the available capacity of the host to receive eggs from fertilized fertile female, with A being the carrying capacity of the host and φ is eggs conversion rate. If the transfer rate of egg to larvae is λ_1 and ω_1 is natural mortality rate of egg stage at temperature τ_1 then, the general equation that describes the egg stage is given by equation 2:

$$\frac{dE_f(t)}{dt} = rF_{ff}(t)\left(1 - \frac{E_f(t)}{A}\right) S_h(t) - (\lambda_1 + \tau_1\omega_1)E_f(t) \tag{2}$$

Larval stage is the most damaging stage of FCM, since larvae can burrow into the fruit and cause damage inside the fruit with few symptoms being displayed on the fruit. The damaged fruit can became vulnerable to secondary pest such as fungal organisms and scavengers (Boardman *et al*., 2012). If ω_2 is the natural mortality rate of larvae at temperature τ_2, and λ_2 is the rate at which larvae turn to pupae. Then, by letting a to denote the conversion efficiency of the larvae, that is the contribution of larval population from susceptible host. Then, the process that describe the fertile larval stage compartment is given by equation 3:

$$\frac{dL_f(t)}{dt} = \lambda_1 E_f(t) + \frac{a\xi S_h(t) L_f(t)}{m + S_h(t)} - (\lambda_2 + \tau_2\omega_2)L_f(t) \tag{3}$$

Once the final instar larva is ready to pupate, it drops to the ground, spins a cocoon and pupates in the top layer of the soil (Boardman *et al*., 2012). At early pupal stage it becomes inactive and can take longer time in development depending on the temperature and humidity of the area (Stibick *et al*., 2008). After maturity at the pupal stage, the male pupae and female pupae can be distinctively identified (Blomefield *et al*., 1989; Stibick *et al*., 2008). Since the transfer rate from larval stage to pupal stage is λ_2, then, by letting ω_3 to be the mortality rate at the pupal stage at temperature τ_3 and λ_3 to be the transfer rate from pupal stage to adult FCM. Then, the equations describing the pupal stage is given by equation 4:

$$\frac{dP_f(t)}{dt} = \lambda_2 L_f(t) - (\omega_3 + \tau_3\lambda_3)P_f(t) \tag{4}$$

After emergence from pupal stage, it is assumed that the fertile female FCM can mate successfully with fertile male FCM in order to move to fertilized fertile female compartment at a rate of λ_4 and after mating, the fertilized fertile female return to fertile female FCM compartment at the rate denoted by δ_1 in order to mate again. Since the transfer rate from larval stage to pupal stage is λ_3, and, by letting κ to be the fraction of pupal population that move to fertile female stage (F_f), and assuming that the natural mortality of fertile female is ω_4 at temperature τ_4 , then, the equation that describes the fertile female compartment is modeled as in equation 5:

$$\frac{dF_f(t)}{dt} = \kappa\lambda_3 P_f(t) + \delta_1 F_{ff}(t) - [\lambda_4 + \tau_4 \omega_4] F_f(t) \quad (5)$$

If the transfer rate of pupal stage to fertile male FCM is λ_4 and $(1 - \kappa)$ is the fraction of pupal population that move to the fertile male stage. Assuming that the natural mortality of the fertile male FCM at temperature τ_5 is given by ω_5 and in fertile male compartment there is no further transfer and the only population reduction of fertile male is due to natural death. Then, the equation that governs adult male compartment is described by equation 6:

$$\frac{dM_f(t)}{dt} = (1 - \kappa)\lambda_3 P_f(t) - \tau_5 \omega_5 M_f(t) \quad (6)$$

For mating to occur female FCM calls the male FCM through pheromone release starting several hours after dark (Stibick *et al*., 2008), the sex pheromone helps the male FCM to allocate themselves in space and time for the available mate (Witzgall *et al*., 2010). Since mating of FCM is a complex process, it is assumed that male FCM can mate several times per day and throughout all its life time. Typically, fertilized fertile female is the one responsible for causing direct damage to the host after laying fertile eggs that hatch and burrow into the host fruit. It is also assumed that fertile female FCM need to mate with a fertile male FCM in order to pass into the fertilized fertile female FCM compartment. If λ_4 is the number of female FCM that move to fertilized fertile female FCM compartment and δ_1 the number of fertilized fertile females that goes back to fertile female compartment for mating again and if the natural mortality rate of fertilized fertile female at temperature τ_6 is given by ω_6. Then, the equation that describes the rate of change at the fertilized fertile female FCM compartment is given equation 7:

$$\frac{dF_{ff}(t)}{dt} = \lambda_4 F_f(t) - (\delta_1 + \tau_6 \omega_6) F_{ff}(t) \quad (7)$$

2.1 Model Flow Chart

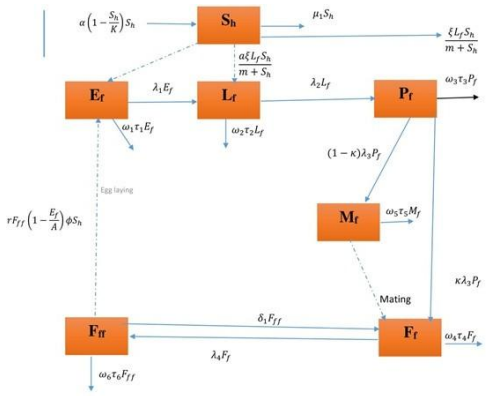

Figure 1: Model Flow Chart

2.2 Model Equation

Taking into account the above considerations, we have the schematic flow diagram shown in Figure 1 (Model Flow Chart). From figure 1, the model will be governed by the following system of equations 8:

$$\begin{aligned}
\frac{dS_h(t)}{dt} &= \alpha\left(1-\frac{S_h(t)}{K_h}\right)S_h(t) - \frac{\xi S_h(t)L_f(t)}{m+S_h(t)} - \mu_1 S_h(t)\\
\frac{dE_f(t)}{dt} &= rF_{ff}(t)\left(1-\frac{E_f(t)}{A}\right) - \varphi S_h(t) - (\lambda_1+\tau_1\omega_1)E_f(t)\\
\frac{dL_f(t)}{dt} &= \lambda_1 E_f(t) + \frac{\alpha\xi S_h(t)L_f(t)}{m+S_h(t)} - (\lambda_2+\tau_2\omega_2)L_f(t)\\
\frac{dP_f(t)}{dt} &= \lambda_2 L_f(t) - (\omega_3+\tau_3\lambda_3)P_f(t)\\
\frac{dF_f(t)}{dt} &= \kappa\lambda_3 P_f(t) + \delta_1 F_{ff}(t) - [\lambda_4+\tau_4\omega_4]F_f(t)\\
\frac{dM_f(t)}{dt} &= (1-\kappa)\lambda_3 P_f(t) - \tau_5\omega_5 M_f(t)\\
\frac{dF_{ff}(t)}{dt} &= \lambda_4 F_f(t) - (\delta_1+\tau_6\omega_6)F_{ff}(t)
\end{aligned} \tag{8}$$

Parameter Values

Symbol	Parameter	Value	Source
α	Intrinsic growth rate of the host	2.76 mm per Month	Verreynne, (2009)
K_h	Environmental carrying capacity	1000-1500 fruits per tree	Assumed
A	Fruit carrying capacity of eggs	3-8 eggs per fruit	Mondaca *et al*., (2020)
β_1	Infestation rate of the pest	0.417-0.5417	Mondaca *et al*., (2020)
λ_1	Transfer rate of E_f to L_f	0.06-0.217	Potgieter, (2013)
λ_2	Transfer rate from L stage to P_m	0.01031-0.05025	Potgieter, (2013)
λ_3	Transfer rate from P to fertile adult moth	0.026-0.164	Potgieter, (2013)
λ_5	Transfer rate of F_f to fertile F_{ff}	0.33	Anguelove *et al*., (2016)
ω_1	Mortality rate of fertile E	0.03	Potgieter, (2013)
ω_2	Mortality rate of fertile L	0.009-0.115	Potgieter, (2013)
ω_3	Mortality rate of fertile Pupa	0.007	Potgieter, (2013)
ω_4	Mortality rate of F_f	0.5	Patinvoh and Susu, (2014)
ω_5	Mortality rate of M_f	0.2	Potgieter, (2013)
ω_6	Mortality rate of F_{ff}	0.2	Potgieter, (2013)
ξ	Harvesting rate of the host	0.06	Assumed
r	Intrinsic egg laying rate	$4.725\text{day}^{-1}\text{female}^{-1}$	Potgieter, (2013)
m	Half saturation constant	0.8	Bhattacharyya and Mukhopadhyay (2014)

Table 1: Parameter values of FCM

3 Equilibria Analysis

All the feasible solutions of model system enters the region $\Omega = \{(S_h(t), E_f(t), L_f(t), P_f(t), F_f(t), M_f(t), F_f f(t))R_+^7 : N(t)\kappa/q(\alpha+1) + \xi$ for all $\xi > 0$ and $t \to 0$. Therefore the system 8 is considered to be positively invariant and attracting and it is sufficient to consider solutions in Ω . The existence, uniqueness and continuation results of system 8 hold in the region and all solutions starting in Ω remain in there for all $t \geq 0$. Hence system 8 is considered to be mathematically well posed and it's sufficient to consider the dynamics the flow generated by the model system 11 in Ω. Also all parameter and state variables for the model system 8 in Ω are assumed to be non-negative since

it monitors plants and pests populations. In this study, we consider three equilibrium point of interest: pest free equilibrium (E_0), coexistence equilibrium (E_2) and host free equilibrium (E_1).

3.1 Pest Free Equilibrium Point

At the pest-free equilibrium points (E_0), it is assumed that there is no pest prevalence in the system hence the population of the host grows logistically to maturity till harvesting time. To analyse pest-free equilibrium point (PFE) the system model 8 the pest components is set to zero, such that: $E_f^* = 0, L_f^* = 0, P_f^* = 0, F_f^* = 0, M_f^* = 0, F_{ff}^* = 0$. This is achieved by setting the right-hand sides of the host pest interaction model 8 equations to zero, given by:

$$E_0 = S_h^*, E_f^*, L_f^*, P_f^*, F_f^*, M_f^*, F_{ff}^*$$

If $(E_f^* = 0, L_f^* = 0, P_f^* = 0, F_f^* = 0, M_f^* = 0, F_{ff}^* = 0$, then, the equations representing the pest compartment reduces to zero. We now solve the first equation of the system model 8 which reduces to equation 9:

$$0 = \alpha' \left(1 - \frac{S_h^*(t)}{K_h}\right)' S_h^*(t) - \frac{\xi S_h^*(t) L_f^*(t)}{m + S_h^*(t)} - \mu_1 S_h^*(t) \tag{9}$$

It is important to note that when $S_h^*(t) = 0$, then we have a trivial solution. Therefore we settle for the second solution $S_h^* = K_h(\alpha - \mu_1)$ to represent the solution of S_h^* in the absence of pest. Consequently, the pest free equilibrium points is given by equation 10:

$$E_0 = (K_h(\alpha - \mu_1), 0, 0, 0, 0, 0) \tag{10}$$

Figures 2 and 3 show numerical simulations used to verify the analytical result of PFE point in equation 10. In Figure 2 the susceptible host population increases sharply to the susceptible host carrying capacity ($K_h = 1000$). This clearly indicates that in the absence of pest and when the harvesting term is set to zero there exist an equilibrium point at the carrying capacity of the susceptible host.

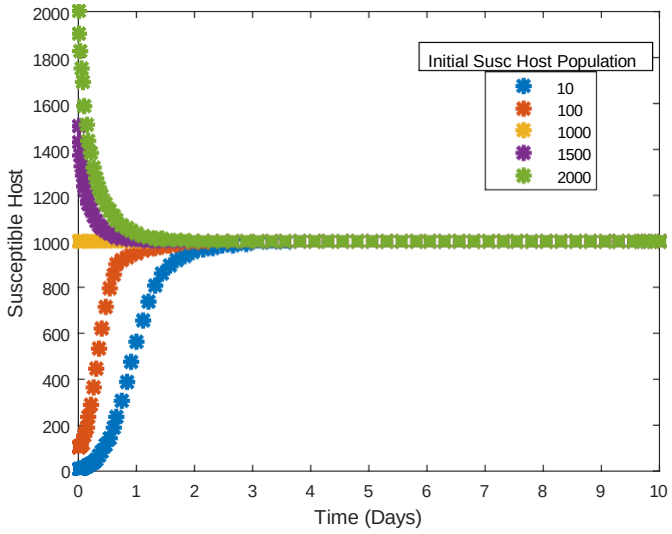

Figure 2: Pest Free Equilibrium with Zero Harvesting Term ($\mu_1 = 0$)

When the harvesting term is introduced in the system, The numerical simulations shows the PFE points is disturbed, and lowers slightly near the susceptible host carrying capacity as illustrated in Figure 3. This further reveals that PFE point is not static and can easily be affected by other human and environmental factors.

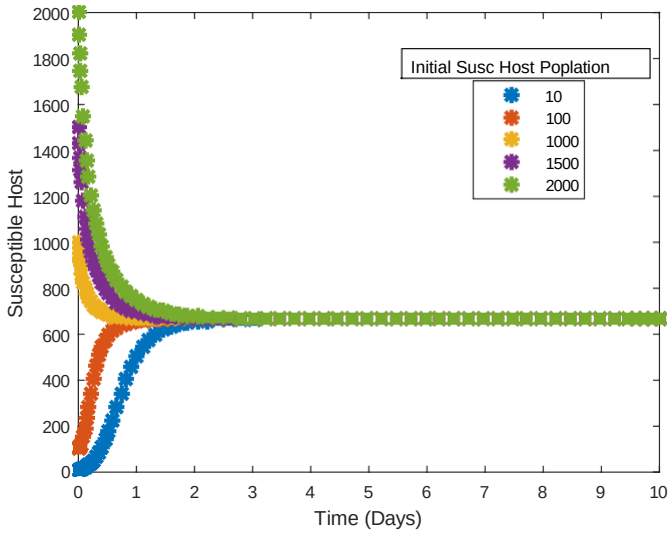

Figure 3: Pest Free Equilibrium with Harvesting Term ($\mu_1 = 0.9$)

3.2 Host Free Equilibrium Points

At this equilibrium point E_2, it is assumed that that the host is absent with the existence FCM pest in the presence of pheromone traps and sterile insect such that, $S_h^{\&} = 0$, $E_f^{\&} /= 0$, $L_f^{\&} /= 0$, $P_f^{\&} /= 0$, $F_f^{\&} /= 0$, $M_f^{\&} /= 0$, $F_{ff}^{\&} /= 0$.

$$\begin{aligned} 0 &= (\lambda_1 + \tau_1\omega_1)E_f^{\&}(t) \\ 0 &= \lambda_1 E_f^{\&}(t) - (\lambda_2 + \tau_2\omega_2)L_f^{\&}(t) \\ 0 &= \lambda_2 L_f^{\&}(t) - (\lambda_3 + \tau_3\omega_3)P_f^{\&}(t) \\ 0 &= \kappa\lambda_3 P_f^{\&}(t) + \delta_1 F_{ff}^{\&}(t) - [\lambda_4 + \tau_4\omega_4]\, F_f^{\&}(t) \\ 0 &= (1-\kappa)\lambda_3 P_f^{\&}(t) - [\tau_5\omega_5]\, M_f^{\&}(t) \\ 0 &= \lambda_4 F_f^{\&}(t) - (\delta_1 + \tau_6\omega_6(t))\, F_{ff}^{\&}(t) \end{aligned} \tag{11}$$

Solving first equation of the equation system 11, it is easy to see that $E_f^{\&} = L_f^{\&} = P_f^{\&} = F_f^{\&}$, $M_f^{\&} = F_{ff}^{\&} = 0$.

Therefore, the host free equilibrium can be given by equation 12:

$$E_2 = (0, 0, 0, 0, 0, 0, 0) \tag{12}$$

From equation 12 it is evidence that at host free equilibrium the pest population become zero. Numerical simulation illustrated in Figure 4, from the Figure it is shown that the total population of reduces to zero irrespective of the initial FCM population showing that the population of FCM become extinct because their survival depends on the availability of the susceptible host.

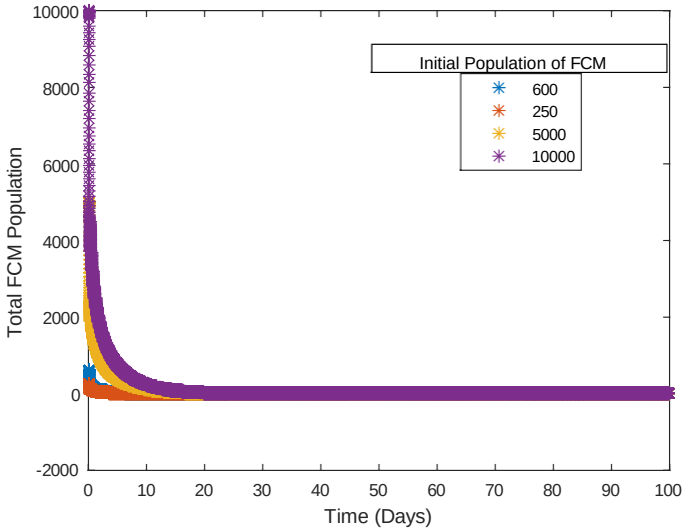

Figure 4: FCM Population against Time at Host Free Equilibrium

In this study, the host free equilibrium point is considered trivial, therefore it is not subjected to stability analysis.

3.3 Coexistence Equilibrium Points

In the presence of FCM and the host, we assume that $S_h \geq 0, E_f \geq 0, L_f \geq 0, P_f \geq 0, F_f \geq 0, M_f \geq 0, F_{ff} \geq 0$. The system model has an equilibrium point called coexistence equilibrium point denoted by $E_2 = (S_h^{*\&}, E_f^{*\&}, L_f^{*\&}, P_f^{*\&}, F_f^{*\&}, M_f^{*\&}, F_{ff}^{*\&})$.

E_2 is the steady state solution where FCM coexist naturally in the population of susceptible host. This is achieved by setting the right-hand sides of the host pest interaction model 8 equations to zero as shown in equation 13, and solving for the values of $S_h^{*\&}, E_f^{*\&}, L_f^{*\&}, P_f^{*\&}, F_f^{*\&}, M_f^{*\&}, F_{ff}^{*\&}$.

$$
\begin{aligned}
0 &= \alpha \left(1 - \frac{S_h^{*\&}(t)}{K_h}\right) S_h^{*\&}(t) - \frac{\xi S_h^{*\&}(t) L_f^{*\&}(t)}{m + S_h^{*\&}(t)} - \mu_1 S_h^{*\&}(t) \\
0 &= rF_{ff}^{*\&}(t)\left(1 - \frac{E_f^{*\&}(t)}{A}\right) S_h^{*\&}(t) - (\lambda_1 + \tau_1\omega_1)E_f^{*\&}(t) \\
0 &= \lambda_1 E_f^{*\&}(t) + \frac{a\xi S_h^{*\&}(t) L_f^{*\&}(t)}{m + S_h^{*\&}(t)} - (\lambda_2 + \tau_2\omega_2)L_f^{*\&}(t) \\
0 &= \lambda_2 L_f^{*\&}(t) - (\lambda_3 + \tau_3\omega_3)P_f^{*\&}(t) \\
0 &= \kappa\lambda_3 P_f^{*\&}(t) + \delta_1 F_{ff}^{*\&}(t) - [\lambda_4 + \tau_4\omega_4] F_f^{*\&}(t) \\
0 &= (1-\kappa)\lambda_3 P_f^{*\&}(t) - \tau_5\omega_5 M_f^{*\&}(t) \\
0 &= \lambda_4 F_f^{*\&}(t) - (\delta_1 + \tau_6\omega_6(t)) F_{ff}^{*\&}(t)
\end{aligned}
\tag{13}
$$

Solving first equation of the equation system 13, we proceed as shown in equation 14:

$$\begin{aligned}
\alpha\left(1-\frac{S_h^{*\&}(t)}{K_h}\right)S_h^{*\&}(t)-\frac{\xi S_h^{*\&}(t)L_f^{*\&}(t)}{m+S_h^{*\&}(t)}-\mu_1 S_h^{*\&}(t)&=0\\
\alpha\left(1-\frac{S_h^{*\&}(t)}{K_h}\right)-\frac{\xi L_f^{*\&}(t)}{m+S_h^{*\&}(t)}-\mu_1&=0\\
\alpha\left(1-\frac{S_h^{*\&}(t)}{K_h}\right)(m+S_h^{*\&}(t))-\xi L_f^{*\&}-\mu_1(m+S_h^{*\&}(t))&=0\\
(S_h^{*\&})^2+\left(\mu_1+\frac{m}{K_h}-\alpha\right)K_h S_h^{*\&}+(\xi L_f^{*\&}+\mu m-\alpha m)K_h&=0
\end{aligned} \tag{14}$$

Therefore, the solution of $S_h^{*\&}(t)$ is given in equation 15:

$$S_h^{*\&}(t)=-\frac{1}{2}\left(\mu_1+\frac{m}{K_h}-\alpha\right)K_h\pm\sqrt{\left(\mu_1+\frac{m}{K_h}-\alpha\right)-4(\xi L_f^{*\&}+\mu m-\alpha m)K_h} \tag{15}$$

Similarly, solving the second equation of equation 13, we proceed as shown in equation 16:

$$\begin{aligned}
rF_{ff}^{*\&}(t)\left(1-\frac{E_f^{*\&}(t)}{A}\right)S_h^{*\&}(t)-(\lambda_1+\tau_1\omega_1)E_f^{*\&}(t)&=0\\
rF_{ff}^{*\&}(t)S_h^{*\&}(t)-\frac{rF_{ff}^{*\&}(t)S_h^{*\&}(t)}{A}E_f^{*\&}(t)-(\lambda_1+\tau_1\omega_1)E_f^{*\&}(t)&=0
\end{aligned} \tag{16}$$

Therefore, the solution of $E_f^{*\&}(t)$ is given in equation 17:

$$E_f^{*\&}(t)=\frac{ArF_{ff}^{*\&}(t)S_h^{*\&}(t)}{rF_{ff}^{*\&}(t)S_h^{*\&}(t)+A(\lambda_1+\tau_1\omega_1)} \tag{17}$$

Similar procedure can be followed to get the solutions of $L_f^{*\&}$, $P_f^{*\&}$, $F_f^{*\&}$, $M_f^{*\&}$, $F_{ff}^{*\&}$ as given in equation 18 :

$$\begin{aligned}
L_f^{*\&}&=\frac{\lambda_1 E_f^{*\&}}{(\lambda_2+\tau_2\omega_2)\left(\lambda_2+\tau_2\omega_2-\frac{a\xi S_h^{*\&}}{m+S_h^{*\&}}\right)}\\
P_f^{*\&}&=\frac{\lambda_2 L_f^{*\&}}{(\lambda_3+\tau_3\omega_3)}\\
F_f^{*\&}&=\frac{\kappa\lambda_3 P_f^{*\&}+\delta_1 F_{ff}^{*\&}}{\tau_4\omega_4+\lambda_4}\\
M_f^{*\&}&=\frac{(1-\kappa)\lambda_3 P_f^{*\&}}{\tau_5\omega_5}\\
F_{ff}^{*\&}&=\frac{\lambda_4 M_f^{*\&}F_f^{*\&}}{(\delta_1+\tau_6\omega_6)}
\end{aligned} \tag{18}$$

The analytical solution for equation 18 is not easy to find. Therefore, we adopt numerical solutions from MATLAB software illustrated in Figures 5 and 6. Figure 5 illustrates the dynamic of susceptible host population with time at the coexistence equilibrium. From the Figure is seen that the equilibrium point is reached at a value lower than the carrying capacity of the susceptible host. This shows the effect of FCM infestation on the susceptible host population.

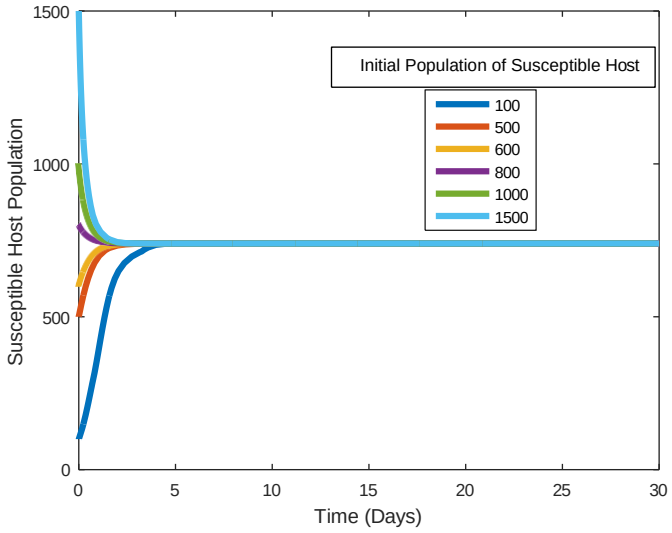

Figure 5: Susceptible Host Population against Time at Coexistence Equilibrium

Figure 6 shows an illustration of total pest population against time in the absence of the control measure at coexistence equilibrium point using the parameter values in Table 1. Using 600 as initial FCM population. From the Figure it is observed that the population in FCM increases sharply to the maximum value, then drops and eventually stabilizes at a value higher than zero.

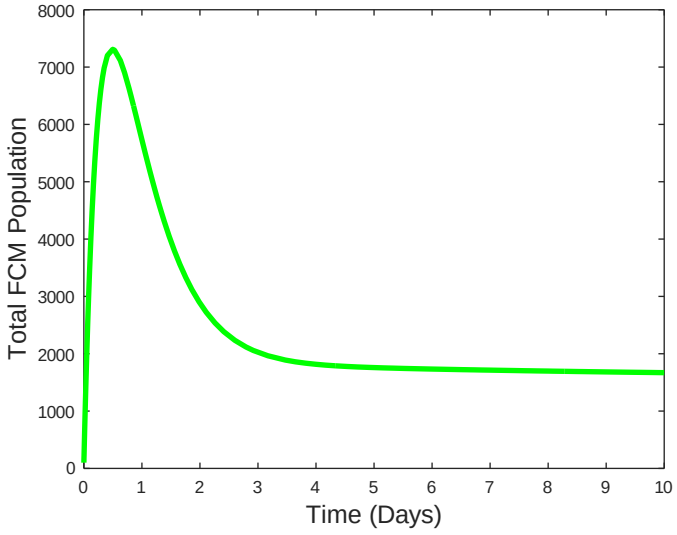

Figure 6: Total FCM Population against Time at Coexistence Equilibrium without control

4 Basic Offspring Number

In this study, we define offspring reproduction number as the average number of fertile eggs laid by a fertilized fertile female in its lifetime when introduced in a completely susceptible host environment with the susceptible host at its carrying capacity. We calculate the basic offspring number following the method used to calculate the basic reproduction number as proposed by Anguelove *et al*. (2016) and Lui and Dai, (2018). Assuming that the FCM is resident within the host population, and since the larval stage is the attacking stage. Using the method of van den Driessch and Watmough (Anguelove *et al*., 2016; Okongo, 2016; Van den Driessche & Watmough, 2002), the offspring reproduction number for the model system 8 can be computed using next generation matrix method. In this case, we consider FCM compartments which are responsible for reproduction of offspring, in such a case the system model 8 is reordered and reduces to equation 19:

$$\begin{aligned}
\frac{dL_f(t)}{dt} &= \lambda_1 E_f(t) + \frac{a\xi S_h(t) L_f(t)}{m + S_h(t)} - (\lambda_2 + \tau_2 \omega_2) L_f(t) \\
\frac{dP_f(t)}{dt} &= \lambda_2 L_f(t) - (\lambda_3 + \tau_3 \omega_3) P_f(t) \\
\frac{dF_f(t)}{dt} &= \kappa \lambda_3 P_f(t) + \delta_1 F_{ff}(t) - [\lambda_4 + \tau_4 \omega_4] F_f(t) \\
\frac{dM_f(t)}{dt} &= (1 - \kappa)\lambda_3 P_f(t) - \tau_5 \omega_5 M_f(t) \\
\frac{dF_{ff}(t)}{dt} &= \lambda_4 F_f(t) - (\delta_1 + \tau_6 \omega_6(t)) F_{ff}(t) \\
\frac{dE_f(t)}{dt} &= rF_{ff}(t) \left(1 - \frac{E_f(t)}{A}\right) \varphi S_h(t) - (\lambda_1 + \tau_1 \omega_1) E_f(t)
\end{aligned} \tag{19}$$

Let $\mathrm{F}_i(y)$ be recruitment rate of new individuals in compartment i, $\mathrm{V}_i^-(y)$ the transfer of individuals out of the compartment i and $\mathrm{V}_i^+(y)$ the transfer of individuals into the compartment i. Then, the system model 19 can be rewritten as shown in equation 20:

$$\frac{dy}{dt} = \mathrm{F}_i(y) - \mathrm{V}_i(y) \tag{20}$$

Where $i = 1, \ldots 6$ and $\mathrm{V}_i(y) = \mathrm{V}_i^-(y) - \mathrm{V}_i^+(y)$. With $\mathrm{F}_i(y)$ and $\mathrm{V}_i(y)$ forms the matrices 21 and 22 respectively:

$$\mathrm{V}_i = \begin{pmatrix} (\lambda_2 + \tau_2\omega_2)L_f(t) \\ -\lambda_2 L_f(t) + (\lambda_3 + \tau_3\omega_3)P_f(t) \\ -\kappa\lambda_3 P_f(t) - \delta_1 F_{ff}(t) + [\lambda_4 + \tau_4\omega_4]\, F_f(t) \\ -(1-\kappa)\lambda_3 P_f(t) + \tau_5\omega_5 M_f(t) \\ -\lambda_4 F_f(t) + (\delta_1 + \tau_6\omega_6(t))\, F_{ff}(t) \\ -rF_{ff}(t)\left(1 - \frac{E_f(t)}{A}\right)\varphi S_h(t) + (\lambda_2 + \tau_2\omega_2)L_f(t) \end{pmatrix} \tag{21}$$

and

$$\mathrm{F}_i = \begin{pmatrix} \lambda_1 E_f(t) + \frac{a\xi S_h(t) L_f(t)}{m + S_h(t)} \\ 0 \\ 0 \\ 0 \\ 0 \\ 0 \end{pmatrix} \tag{22}$$

To obtain the next generation operator, we compute the Jacobian Matrices of F_i and V_i and solve it at the PFE with $E_0 = (K_h(\alpha - \mu_1), 0, 0, 0, 0, 0, 0)$ denoted by F and V respectively. Consequently, the basic offspring number of the system model 8 is obtained by determining the spectral radius of the matrix FV^{-1} as given in the equation 23:

$$\mathrm{R}_0 = \frac{a\xi K_h(\alpha - \mu_1)}{(m + K_h(\alpha - \mu_1))(\lambda_2 + \tau_2\omega_2)} \tag{23}$$

It measures the mean number of new offspring produced by fertilized fertile female in the completely susceptible host population at its carrying capacity. By substituting the parameter values from Table 1 in the equation 23, the basic reproduction number is found to be less than unity. Since the basic reproduction number R_0 is less than unity, there is likelihood of pest infestation in the susceptible host reducing.

5 Stability Analysis

In this section, the local stability of the equilibrium points of the model system 8 is investigated. In order to perform the local stability analysis of the model system 8 around the equilibrium points E_0 and E_2.

5.1 Local Stability Analysis

To perform the local stability analysis of the model system 8, we proceed by constructing the Jacobian matrix of the model system 8 and solving it at the equilibrium points. If the eigenvalues are positive real parts then the equilibrium points are unstable, but if the eigenvalues are negative real parts then, the equilibrium points are stable. The system 8 can be written in vector form as given in equation 24:

$$\frac{dy}{dt} = f(y) \tag{24}$$

where:

$$y = (S_h(t), E_f(t), L_f(t), P_f(t), F_f(t), M_f(t), F_{ff}(t))$$

Then, the function y can be written in matrix form as shown in equation 25:

$$f(y) = \begin{bmatrix} \alpha\left(1 - \frac{S_h(t)}{K_h}\right) S_h(t) - \frac{\xi S_h(t) L_f(t)}{m+S_h(t)} - \mu_1 S_h(t) \\ rF_{ff}(t)\left(1 - \frac{E_f(t)}{A}\right) \varphi S_h(t) - (\lambda_1 + \tau_1\omega_1)E_f(t) \\ \lambda_1 E_f(t) + \frac{a\xi S_h(t) L_f(t)}{m+S_h(t)} - (\lambda_2 + \tau_2\omega_2)L_f(t) \\ \lambda_2 L_f(t) - (\lambda_3 + \tau_3\omega_3)P_f(t) \\ \kappa\lambda_3 P_f(t) + \delta_1 F_{ff}(t) - [\lambda_4 + \tau_4\omega_4]\, F_f(t) \\ (1-\kappa)\lambda_3 P_f(t) - [\tau_5\omega_5]\, M_f(t) \\ \lambda_4 F_f(t) - (\delta_1 + \tau_6\omega_6(t))\, F_{ff}(t) \end{bmatrix} \tag{25}$$

Clearly, the right hand side of equation 25 is continuous and locally Lipschitz, so uniqueness and local existence of the solution is guaranteed. By computing the Jacobian matrix of equation 25 yields equation 26:

$$\mathbf{J}_f = \begin{bmatrix} x_1 & 0 & x_2 & 0 & 0 & 0 & 0 \\ x_3 & x_4 & 0 & 0 & 0 & 0 & x_5 \\ x_6 & x_7 & x_8 & 0 & 0 & 0 & 0 \\ 0 & 0 & x_9 & x_{10} & 0 & 0 & 0 \\ 0 & 0 & 0 & x_{11} & x_{12} & 0 & x_{14} \\ 0 & 0 & 0 & x_{17} & 0 & x_{19} & 0 \\ 0 & 0 & 0 & 0 & x_{21} & 0 & x_{23} \end{bmatrix} \tag{26}$$

Where: $x_1 = \alpha - \frac{2S_h}{K_h} - \frac{\xi L_f (m+S_h) - \xi S_h L_f}{(m+S_h)^2} - \mu_1$, $x_2 = -\frac{\xi S_h}{m+S_h}$, $x_3 = rF_{ff}\left(1 - \frac{E_f}{A}\right)\varphi$, $x_4 = -\frac{rF_{ff}S_h}{A} - (\lambda_1 + \tau_1\omega_2)$, $x_5 = rS_h$, $x_6 = \frac{a\xi L_f}{(m+S_h)^2}$, $x_7 = \lambda_1$, $x_8 = \frac{a\xi S_h}{m+S_h} - (\lambda_2 + \tau_2\omega_2)$, $x_9 = \lambda_2$, $x_{10} = -(\lambda_3 + \tau_3\omega_3)$, $x_{11} = \kappa\lambda_3$, $x_{12} = -(\lambda_4 - \tau_4\omega_4)$, $x_{13} = 0$, $x_{14} = \delta_1$, $x_{17} = (1-\kappa)\lambda_3$, $x_{19} = -\tau_5\omega_5$, $x_{20} = 0$, $x_{21} = \lambda_4$, $x_{23} = -(\delta_1 + \tau_6\omega_6)$. The Jacobian matrix 26 is evaluating at both the pest free and coexistence equilibrium points that is E_0 and E_1, if the eigenvalues are found to be all positive then, the equilibrium point is said to be unstable equilibrium point but if all the eigenvalues are negative then then, the equilibrium point is said to be stable equilibrium point.

Theorem 1. *The PFE point E_0 is locally asymptotically stable if $R_0 < 1$ and otherwise unstable*

Proof. The local stability analysis of the model system 8 can be determined by solving the jacobian matrix 26 at the pest free equilibrium points ($E_0 = (K_h(\alpha - \mu_1), 0, 0, 0, 0, 0, 0)$, which yields equation 27:

$$\mathbf{J}_f|E_0 = \begin{bmatrix} x_1 & 0 & x_2 & 0 & 0 & 0 & 0 \\ 0 & 0 & x_4 & 0 & 0 & 0 & x_5 \\ 0 & x_7 & x_8 & 0 & 0 & 0 & 0 \\ 0 & 0 & x_9 & x_{10} & 0 & 0 & 0 \\ 0 & 0 & 0 & x_{11} & x_{12} & 0 & x_{13} \\ 0 & 0 & 0 & x_{14} & 0 & x_{15} & 0 \\ 0 & 0 & 0 & 0 & x_{16} & 0 & x_{17} \end{bmatrix} \tag{27}$$

Where: $x_1 = \mu_1 - \alpha$, $x_2 = -\frac{\xi Kh(\alpha-\mu 1)}{m+K_h(\alpha-\mu_1)} = -R_0\frac{(\lambda 2+\tau 2\omega 2)}{a}$, $x_4 = -(\lambda_1 + \tau_1\omega_2)$, $x_5 = rK_h(\alpha - \mu_1)$, $x_7 = \lambda_1$, $x_8 = \frac{a\xi K_h(\alpha-\mu_1)}{m+K_h(\alpha-\mu_1)} - (\lambda_2 + \tau_2\omega_2) = (\lambda_2 + \tau_2\omega_2)(R_0 - 1)$, $x_9 = \lambda_2$, $x_{10} = -(\lambda_3 + \tau_3\omega_3)$, $x_{11} = \kappa\lambda_3$, $x_{12} = -\tau_4\omega_4$, $x_{13} = \delta_1$, $x_{14} = (1 - \kappa)\lambda_3$, $x_{15} = -[\tau_3\omega_3]$, $x_{16} = \lambda_4$, $x_{17} = -(\delta_1 + \tau_6\omega_6)$. The matrix 27 is solved using the Wolfram mathematica software, an extract of the solution is as given by the following equation:

$s_1 = x_1$, $s_2 = x_{15}$, $s_3 = s_4 = s_6 = s_7 = [x_{10}x_{13}x_{16}x_4x_8 - x_{10}x_{12}x_{17}x_4x_8 - x_{11}x_{16}x_5x_7x_9 + (-x_{10}x_{13}x_{16}x_4 + x_{10}x_{12}x_{17}x_4 - x_{10}x_{13}x_{16}x_8 + x_{10}x_{12}x_{17}x_8 + x_{10}x_{12}x_4x_8 - x_{13}x_{16}x_4x_8 + x_{10}x_{17}x_4x_8 + x_{12}x_{17}x_4x_8) + (x_{10}x_{13}x_{16} - x_{10}x_{12}x_{17} - x_{10}x_{12}x_4 + x_{13}x_{16}x_4 - x_{10}x_{17}x_4 - x_{10}x_{12}x_4 - x_{10}x_{12}x_8 + x_{13}x_{16}x_8 - x_{10}x_{17}x_8 - x_{12}x_{17}x_8 - x_{10}x_4x_8 - x_{12}x_4x_8 - x_{17}x_4x_8) + (x_{10}x_{12} - x_{13}x_{16} + x_{10}x_{17} + x_{12}x_{17} + x_{10}x_4 + x_{12}x_4 + x_{17}x_4 + x_{10}x_8 + x_{12}x_8 + x_{17}x_8 + x_4x_8) + (-x_{10} - x_{12} - x_{17} - x_4 - x_8)]$ Since all the eigenvalues of the pest free equilibrium are negative, such that if $R_0 < 1$ then the pest free equilibrium point is said to be a stable equilibrium point but if $R_0 > 1$ then the equilibrium point would be unstable . The system 8 is therefore locally asymptotically stable around the pest free equilibrium point ($E_0 = (K_h(\alpha - \mu_1), 0, 0, 0, 0, 0, 0)$. □

Theorem 2. *The coexistence equilibrium point E_1 is locally asymptotically stable if* $R_0 < 1$ *and otherwise unstable*

Proof. The local stability analysis of the model system 8 can be established by solving the Jacobian matrix 26 at the coexistence equilibrium points (E_1) which yields equation 28 :

$$\mathbf{J}_{\mathcal{F}} = \begin{bmatrix} y_1 & 0 & y_2 & 0 & 0 & 0 & 0 \\ y_3 & y_4 & 0 & 0 & 0 & 0 & y_5 \\ y_6 & y_7 & y_8 & 0 & 0 & 0 & 0 \\ 0 & 0 & y_9 & y_{10} & 0 & 0 & 0 \\ 0 & 0 & 0 & y_{11} & y_{12} & 0 & y_{14} \\ 0 & 0 & 0 & y_{17} & 0 & y_{19} & 0 \\ 0 & 0 & 0 & 0 & y_{21} & 0 & y_{23} \end{bmatrix} \tag{28}$$

$$\mathbf{J}_{\mathcal{F}}|E_1 = \begin{bmatrix} y_1 & 0 & y_2 & 0 & 0 & 0 & 0 \\ 0 & x_3 & x_4 & 0 & 0 & 0 & x_5 \\ x_6 & x_7 & x_8 & 0 & 0 & 0 & 0 \\ 0 & 0 & x_9 & x_{10} & 0 & 0 & 0 \\ 0 & 0 & 0 & x_{11} & x_{12} & 0 & x_{13} \\ 0 & 0 & 0 & x_{14} & 0 & x_{15} & 0 \\ 0 & 0 & 0 & 0 & x_{16} & 0 & x_{17} \end{bmatrix} \tag{29}$$

Where: $y_1 = \alpha - \frac{2S_h^{*\&}}{K_h} - \frac{\xi L_f^{*\&}(m+S^{*\&}_h) - \xi S^{*\&}_h L^{*\&}_f}{(m+S^{*\&}_h)^2} - \mu_1$, $y_2 = -\frac{\xi S_h^{*\&}}{m+S_h^{*\&}}$, $y_3 = rF_{ff}^{*\&}\left(1 - \frac{E_f^{*\&}}{A}\right)$, $y_4 = -\frac{rF_{ff}^{*\&}S_h^{*\&}}{A} - (\lambda_1 + \tau_1\omega_2)$, $y_5 = rS_h^{*\&}$, $y_6 = \frac{a\xi L_f^{*\&}}{(m+S_h^{*\&})^2}$, $y_7 = \lambda_1$, $y_8 = \frac{a\xi S_h^{*\&}}{m+S_h^{*\&}} - (\lambda_2 + \tau_2\omega_2)$, $y_9 = \lambda_2$, $y_{10} = -(\lambda_3 + \tau_3\omega_3)$, $y_{11} = \kappa\lambda_3$, $y_{12} = -\tau_4\omega_4$, $y_{14} = \delta_1$, $y_{17} = (1 - \kappa)\lambda_3$, $y_{19} = -\tau_5\omega_5$, $y_{21} = \lambda_4$, $y_{23} = -(\delta_1 + \tau_6\omega_6)$, With the values of $S_h^{*\&}$, $E_f^{*\&}$, $L_f^{*\&}$, $P_f^{*\&}$, $F_f^{*\&}$, $M_f^{*\&}$, $F_{ff}^{*\&}$ are as given in equations 15, 17 and 18. The matrix 28 is solved using the Wolfram mathematica software, which yields the eigenvalues as: $s_1 = y_{15}$, $s_2 = s_3 = s_4 = s_5 = s_6 = s_7 = s_8 = [x_{10}x_{13}x_{16}x_2x_4x_6 - x_{10}x_{12}x_{17}x_2x_4x_6 - x_{10}x_{13}x_{16}x_2x_3x_7 + x_{10}x_{12}x_{17}x_2x_3x_7 - x_1x_{10}x_{13}x_{16}x_4x_8 + x_1x_{10}x_{12}x_{17}x_4x_8 + x_1x_{11}x_{16}x_5x_7x_9 + \ldots]$. Since all the eigenvalues of the coexistence equilibrium points are negative, then the coexistence equilibrium point is a stable equilibrium point. The system 8 is therefore locally asymptotically stable around the the coexistence equilibrium points E_1. □

6 Global Stability Analysis

For population models, global stability should be used in a restricted sense, that is, the definition must be restricted to the feasible region. Such that if a disturbance shift the state of the system to any other feasible state and the system is thereafter left alone, then, the natural dynamics of the system would move the state back into a small neighborhood of the equilibrium. If the disturbance caused the extinction of one species or invasion by a new species, mathematically and biologically the system should be thought of as a new system. Consequently, the equilibrium points, and the stability of the new system will be examined (Goh Nedlands, 1976).

6.1 Global Stability of PFE

To study the global asymptotic stability of the PFE, one common approach is to construct an appropriate Lyapunove function as proposed by Van Den Driessche & Watmough, (2002). However, its simpler to apply the method introduced by Catillo-Chevez *et al*. (2002) and adopted Bhunu and Mushayabasa, (2014). Therefore, we study the global stability of the system model 8 around pest free equilibrium point (E_0). Assuming the system is cooperative on R^7_+, such that the growth in any compartment impact positively on the growth of all other compartment. We investigate the global asymptotic stability of the pest free equilibrium using the theorem of Catillo-Chevez *et al*. (2002), by rewriting the system 8 in the form shown in equation 29:

$$\begin{aligned} \frac{dX}{dt} &= F(X, Z) \\ \frac{dZ}{dt} &= G(X, Z),\ G(X, 0) = 0 \end{aligned} \tag{30}$$

Where: $X = (S_h) \in \mathrm{R}^1_+$ denotes noninfectious compartments and $Z = (E_f, L_f, P_f, F_f, M_f, F_{ff},) \in \mathrm{R}^6_+$ denotes the infectious pest compartments. $E_0 = (X^*, 0)$ represents the pest free equilibrium of the system. If this points satisfies the following conditions: (i) for $\frac{dX}{dt} = F(X, 0)$, where X^* is globally asymptotically stable, (ii) $\frac{dZ}{dt} = D_z G(X, 0)Z - G(X, Z)$, $G(X, Z) \geq 0$ for all $(X, Z) \in \Omega$, then, we can conclude that E_0 is globally asymptotically stable if the following theorem 29 holds:

Theorem 3. *The equilibrium point $E_0 = (X^*, 0)$ of the system 29 is globally asymptotically stable if $\mathrm{R}_0 \leq 1$ and the conditions (i) and (ii) are satisfied.*

Proof. To prove this, we start by defining new variables and dividing the system 8 into sub systems $X = (S_h)$ and $Z = (E_f, L_f, P_f, F_f, M_f, F_{ff})$. From equation 29, we have two vector valued functions $G(X, Z)$ and $F(X, Z)$ given by equations 30 and 31:

$$F(X, Z) = \alpha\left(1 - \frac{S_h(t)}{K_h}\right) S_h(t) - \frac{\xi S_h(t) L_f(t)}{m + S_h(t)} - \mu_1 S_h(t) \tag{31}$$

and

$$G(X, Z) = \begin{bmatrix} rF_{ff}(t)\left(1 - \frac{E_f(t)}{A}\right) S_h(t) - (\lambda_1 + \tau_1\omega_1)E_f(t) \\ \lambda_1 E_f(t) + \frac{a\xi S_h(t) L_f(t)}{m + S_h(t)} - (\lambda_2 + \tau_2\omega_2)L_f(t) \\ \lambda_2 L_f(t) - (\lambda_3 + \tau_3\omega_3)P_f(t) \\ \kappa\lambda_3 P_f(t) + \delta_1 F_{ff}(t) - (\lambda_4 + \tau_4\omega_4)F_f(t) \\ (1 - \kappa)\lambda_3 P_f(t) - \tau_5\omega_5 M_f(t) \\ \lambda_4 F_f(t) - (\delta_1 + \tau_6\omega_6(t))F_{ff}(t) \end{bmatrix} \tag{32}$$

Now, let consider the reduced system, $\frac{dX}{dt} = F(X, 0)$ from condition (i) yields:

$$\frac{dS_h}{dt} = \alpha'\left(1 - \frac{S_h(t)}{K_h}\right)' S_h(t) - \mu S_h(t) \tag{33}$$

We note that this is asymptomatic dynamics system, independence of the initial conditions in D, therefore the convergence of the solutions of the reduced system 32 is global in D. We then compute:

$$G(X, Z) = D_z G(X^*, 0) - \hat{G}(X, Z)$$

and show that

$$\hat{G}(X, Z) \geq 0$$

Now, we let $B = D_z G(X^*, 0)$, which is the Jacobian of $\hat{G}(X, Z)$ taken in $(E_f, L_f, P_f, F_f, M_f, F_{ff})$ and evaluated at $(X^*, 0)$. Such that the matrix B is given by the equation 33:

$$B = \begin{bmatrix} x_1 & 0 & 0 & 0 & 0 & x_2 \\ x_3 & x_4 & 0 & 0 & 0 & 0 \\ 0 & x_5 & x_6 & 0 & 0 & 0 \\ 0 & 0 & x_7 & x_8 & 0 & x_9 \\ 0 & 0 & x_{11} & 0 & x_{12} & 0 \\ 0 & 0 & 0 & 0 & 0 & x_{13} \end{bmatrix} \tag{34}$$

Where: $x_1 = -(\lambda_1 + \tau_1\omega_1)$, $x_2 = -rK_h(\alpha - \mu_1)$, $x_3 = \lambda_1$, $x_4 = \frac{a\xi K h(\alpha - \mu 1)}{m + K_h(\alpha - \mu_1)} - (\lambda_2 + \tau_2\omega_2)$, $x_5 = \lambda_2$, $x_6 = -(\lambda_3 + \tau_3\omega_3)$, $x_7 = \kappa\lambda_3$, $x_8 = -\tau_4\omega_4$, $x_9 = \delta_1$, $x_{10} = \delta_2$, $x_{11} = (1 - \kappa)\lambda_3$, $x_{12} = -[g_1 + \tau_5\omega_5$, $x_{13} = -(\delta_1 + \tau_6\omega_6)$, $x_{14} = \lambda_4$, $x_{15} = -(\delta_2 + \tau_7\omega_7)$.

The value for $\hat{G}(X, Z)$ is given by equation 34:

$$\hat{G}(X, Z) = \begin{matrix} rF_{ff}(t)\ \ 1 - \frac{E_f(t)}{A}\ \ (K_h(\alpha - \mu_1) - S_h(t) \\ \alpha\xi L_f(t)(\frac{(K_h(\alpha-\mu_1)}{m+(K_h(\alpha-\mu_1)} - \frac{S_h}{m+S_h}) \\ 0 \\ 0 \\ 0 \\ 0 \end{matrix} \tag{35}$$

Since $K_h \geq S_h$. it is clear that $\hat{G}(X, Z) \geq 0$ for all $(X, Z) \in \mathrm{D}$, then, the pest-free equilibrium will be globally asymptotically stable. We also notice that the matrix B is an M-matrix since all its off-diagonal elements are non-negative. Therefore, this proves that PFE is globally asymptotically stable. □

The implication of this results is that the pest free equilibrium will be globally asymptotically stable. However, whenever the FCM undergo diapausing the PFE may not be necessarily globally asymptotically stable which is not true from the values of $\hat{G}(X, Z) \geq 0$ everywhere in D which suggests the existence of multiple coexistence equilibria.

6.2 Global Stability Analysis of Coexistence Equilibrium

Theorem 4. *For host-pest interactions model, sufficient condition for global stability are (i) coexistence equilibrium point is feasible, (ii) the equilibrium is a local asymptomatic stable solution.*

Proof. Global stability of coexistence equilibrium points can be constructed using a suitable Lyapunov function an approach adopted by Korobeinikor (2004a) and ullah *et al*. (2013). In this approach Lyapunov function is constructed basing on equation 35:

$$L = \sum a_i(x_i - x_i^{*\&} \ln x_i) \tag{36}$$

Where a_i is the constant selected such that $a_i > 0$, x_i is the population of the *ith* compartment and $x_i^{*\&}$ is the coexistence equilibrium point. Therefore, consider the Lyapunove function in equation 36:

$$\begin{aligned} L =& a_1(S_h - S_h^{*\&} \ln S_h) + a_2(E_f - E_f^{*\&} \ln E_f) + a_3(L_f - L_f^{*\&} \ln L_f) + a_4(P_f - P_f^{*\&} \ln P_f) \\ &+ a_5(F_f - F_f^{*\&} \ln F_f) + a_6(M_f - M_f^{*\&} \ln M_f) + a_7(F_{ff} - F_{ff}^{*\&} \ln F_{ff}) \end{aligned} \tag{37}$$

Differentiating 4.7.8 with respect to time yields equation 37:

$$\begin{aligned}
\frac{dL}{dt} &= a_1\left(1-\frac{S_h^{*\&}}{S_h}\right)\frac{dS_h}{dt} + a_2\left(1-\frac{E_f^{*\&}}{E_f}\right)\frac{dE_f}{dt} + a_3\left(1-\frac{L_f^{*\&}}{L_f}\right)\frac{dL_f}{dt} + a_4\left(1-\frac{P_f^{*\&}}{P_f}\right)\frac{dP_f}{dt} \\
&+ a_5\left(1-\frac{F_f^{*\&}}{F_f}\right)\frac{dF_f}{dt} + a_6\left(1-\frac{M_f^{*\&}}{M_f}\right)\frac{dM_f}{dt} + a_7\left(1-\frac{F_{ff}^{*\&}}{F_{ff}}\right)\frac{dF_{ff}}{dt} \\
&= a_1\left(1-\frac{S_h^{*}}{S_h}\right)\left(\alpha\left(1-\frac{S_h(t)}{K_h}\right)S_h(t) - \frac{\xi S_h(t) L_f(t)}{m+S_h(t)} - \mu_1 S_h(t)\right) \\
&+ a_2\left(1-\frac{E_f^{*\&}}{E_f}\right)\left(rF_{ff}(t)\left(1-\frac{E_f(t)}{A}\right)S_h(t) - (\lambda_1+\tau_1\omega_1)E_f(t)\right) \\
&+ a_3\left(1-\frac{L_f^{*\&}}{L_f}\right)\left(\lambda_1 E_f(t) + \frac{a\xi S_h(t) L_f(t)}{m+S_h(t)} - (\lambda_2+\tau_2\omega_2)L_f(t)\right) \\
&+ a_4\left(1-\frac{P_f^{*\&}}{P_f}\right)\left[\lambda_2 L_f(t) - (\lambda_3+\tau_3\omega_3)P_f(t)\right] \\
&+ a_5\left(1-\frac{F_f^{*\&}}{F_f}\right)\left[\kappa\lambda_3 P_f(t) + \delta_1 F_{ff}(t) - [\lambda_4+\tau_4\omega_4]F_f(t)\right] \\
&+ a_6\left(1-\frac{M_f^{*\&}}{M_f}\right)\left[(1-\kappa)\lambda_3 P_f(t) - \tau_5\omega_5 M_f(t)\right] \\
&+ a_7\left(1-\frac{F_{ff}^{*\&}}{F_{ff}}\right)\left[\lambda_4 F_f(t) - (\delta_1+\tau_6\omega_6(t))F_{ff}(t)\right]
\end{aligned} \tag{38}$$

Where: $S_h(t) = S_h^{*\&}$, $E_f(t) = E_f^{*\&}$, $L_f(t) = L_f^{*\&}$, $P_f(t) = P_f^{*\&}$, $F_f(t) = F_f^{*\&}$, $M_f(t) = M_f^{*\&}$, $F_{ff}(t) = F_{ff}^{*\&}$.

Following McClusky's (2010) approach, and assuming that system model 8 is positively invariant, equation 37 is non-positive. Hence $\frac{dL}{dt} \leq 0 \forall S_h, E_f, L_f, P_f, F_f, M_f, F_{ff} > 0$ and is zero when $S_h(t) = S_h^{*\&}$, $E_f(t) = E_f^{*\&}$, $L_f(t) = L_f^{*\&}$, $P_f(t) = P_f^{*\&}$, $F_f(t) = F_f^{*\&}$, $M_f(t) = M_f^{*\&}$, $F_{ff}(t) = F_{ff}^{*\&}$. Therefore, the largest invariant set in $\{(S_h^{*\&}, E_f^{*\&}, L_f^{*\&}, P_f^{*\&}, F_f^{*\&}, M_f^{*\&}, F_{ff}^{*\&}) \in D\}$ such that $\frac{dL}{dt} = 0$ is the singleton $\{E_1\}$ which is the coexistence equilibrium point. According to the invariant principle put forward by Lasalles, (1976), E_1 is globally asymptotically stable in D, if $R_0 \leq 1$ the interior of D, otherwise unstable. □

This results implies that the elimination of FCM is possible irrespective of the initial sizes of the sub-populations of FCM of the model, whenever the threshold parameter R_0 is less than unity. Therefore, from Lyapunov-LaSella invariance principle, the system model 8 is uniformly persistence.

7 Numerical Simulation

The impact of FCM on the susceptible host is obtained by performing numerical simulations of the system model 8 using parameters on Table 1 and setting the temperature at 20^0. Graphical illustration of the impact of FCM on the susceptible host is shown in Figures 7, 8 and 9. A graph of susceptible host against time for a period of 30 days is illustrated in Figure 7. From the graph the population of the susceptible grows from the FCM initial population of 100 logistically and level off at 428. Since the carrying capacity K_h of the susceptible host is set at 1000, the presence of the FCM pest clearly makes the susceptible host to grow below its carrying capacity. When the FCM initial population is increased to 500 the susceptible host population drops exponentially and again levels off at 428, this is due to the effect of FCM on the population of the susceptible host.

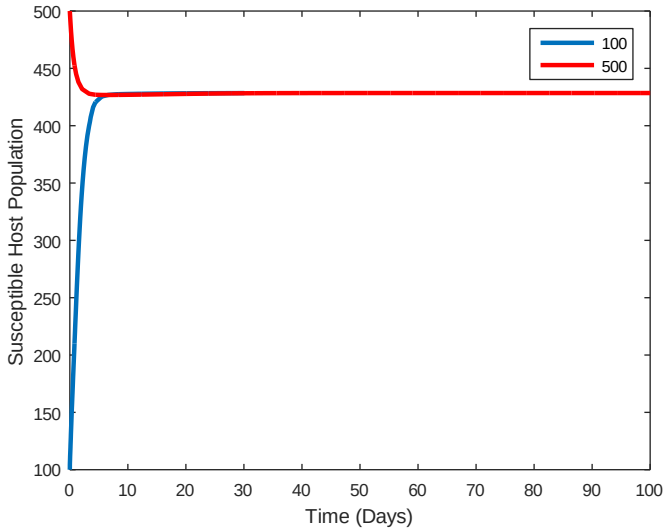

Figure 7: A plot of Susceptible Host against Time

Figure 8 illustrates a graph of FCM total population with time in a period of 30 days. From the graph its observed that the FCM population first sharply increase from the initial population of 1500 to a maximum population of 372099, then starts to drops gradually and levels off at a population of 4272 after 30 day. If the initial population of FCM in the field is reduced to about 100, the population of FCM is observed to rise to a maximum value of 30575, then drops gradually and levels at the minimum value of 1757. The first increase is due to the availability of food for the FCM pest as time goes by the available number of susceptible host starts to decline leading to the decline of the FCM population in the field. The population of the FCM does not drop to zero because the susceptible host is continuously being introduced in the field, under no control.

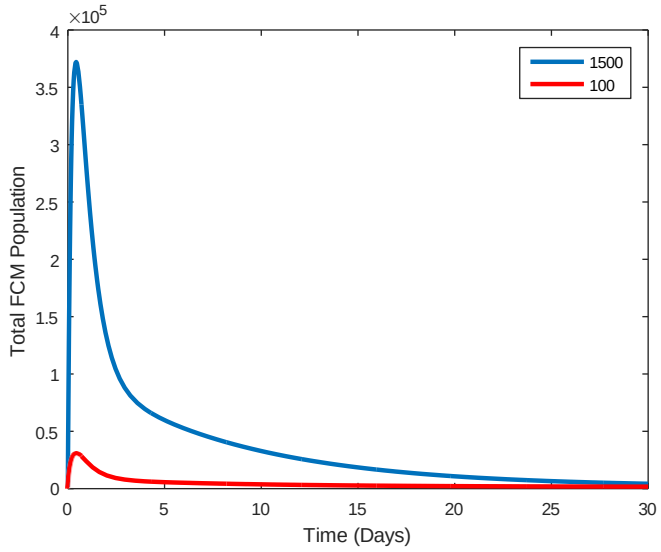

Figure 8: A plot of Total FCM Population against Time

Figure 9 shows a plot of susceptible host with time in the presence of FCM under different susceptible host recruitment rate that is α = 0.2, 1.0, 2.0, 2.5 while leaving other parameters in Table 1 constant. From the Figure it observed that the number of susceptible hosts decrease from the initial number 100 with time and levels off at 0 when the α = 0.2, but when α = 2.5 the susceptible host increase gradually and level off at a values lower than the host's carrying capacity. This shows that at very low α the FCM feeds on the available host until all the host are completely depleted from the population.

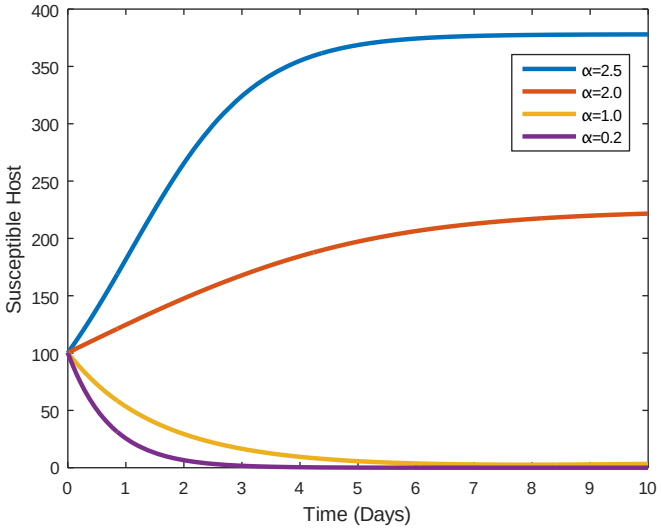

Figure 9: A plot of the Susceptible host with time in the presence of the FCM

8 Discussion and Conclusions

In this paper, deterministic model of FCM interaction with susceptible host is developed and carefully analysed to bring insight into its dynamical features of FCM interaction with the hosts. The model is considered is considered to be biologically and mathematically well posed. Using next generation matrix method the basic reproduction number is obtained. the model was analysed qualitatively and the local and global stability of their associated equilibria. The dynamics of the FCM infestation on the susceptible host population showed that in the absence of any control measures the population of FCM would increase. Consequently leading to decrease of susceptible host population. As the host population reduces FCM at the larval stage continue to lose food, hence their population also starts to decline as illustrated by numerical simulation in Figure 7. From the numerical simulation it can be seen that the presence of FCM in a farm greatly affects the population of susceptible host, hence there is a need to control FCM for better farm produce. This can be done using biological control, or chemical control strategies. Therefore, in our next paper we will by introduce control strategies in our model.

9 Recommendations

In this study, we have only concentrated on the FCM interaction with the susceptible host without including any control measure. Therefore, in our next study area, we shall extend the model to include FCM control strategies. There should be more enlightenment campaign on the economic effects of FCM to crops and identification method of FCM on crops by the farmers.

10 Conflicts of interest

There are no conflicts to declare.

11 Acknowledgments

We thanks the administrative staff in the department of physical science of Chuka University for their hospitality and assistance in matters related to our research work.

References

[1] Alemneh, H. T., Makinde, O. D., and Theuri, D. M. (2019). Mathematical modelling of msv pathogen interaction with pest invasion on maize plant. *Global Journal of Pure and Applied Mathematics*, 15(1):55–79.

[2] Anderson, R. and May, R. (1979). Population Biology of Infectious Diseases: Part I. *Nature*, 280:361–7.

[3] Anguelov,M.R.,Dufourd,C.,andDumont,Y.(2016). MathematicalModelforPest-Insect Control using Mating Disruption and Trapping. *Applied Mathematical Modelling*.

[4] Barclay, H. J. and Haniotakis, G. E. (1991). Combining Pheromone-Baited and Food- Baited Traps for Insect Pest Control: Effects of Developmental Period. Population Ecology, 33(2):269–285.

[5] Barclay, H. J., Steacy, R., Enkerlin, W., and van den Driessche, P. (2016). Modeling Dif- fusive Movement of Sterile Insects Released along Aerial Flight Lines. *International Journal of Pest Management*, 62(3):228–244.

[6] Barclay, H. J. and Van Den Driessche, P. (1990). A sterile Release Model for Control of a Pest with two Life Stages under Predation. *The Rocky Mountain Journal of Mathematics*, pages 847–855.

[7] Bhattacharyya, R. and Mukhopadhyay, B. (2014). Mathematical study of a pest control model incorporating sterile insect technique. *Natural Resource Modeling*, 27(1):61– 79.

[8] Blomefield, T. et al. (1989). Economic Importance of False Codling Moth, Cryptophlebia leucotreta, and Codling Moth, Cydia Pomonella, on Peaches, Nectarines and Plums. Phytophylactica, 21(4):435–436.

[9] Bhunu, C. and Mushayabasa, S. (2011). Modelling the transmission dynamics of pox-like infections. *International Journal of Applied Mathematics*.

[10] Blomefield, T. et al. (1989). Economic Importance of False Codling Moth, Cryptophlebia leucotreta, and Codling Moth, Cydia Pomonella, on Peaches, Nectarines and Plums. Phytophylactica, 21(4):435–436.

[11] Boardman, L., Grout, T. G., and Terblanche, J. S. (2012). False codling moth thaumatotibia leucotreta (lepidoptera, tortricidae) larvae are chill-susceptible. *Insect Science*, 19(3):315–328.

[12] Byers, J. A. (2014). Simulation of Mating Disruption and Mass Trapping with Competitive Attraction and Camouflage. *Environmental Entomology*, 36(6):1328–1338.

[13] Castillo-Chavez, C. and Song, B. (2004). Dynamical models of tuberculosis and their applications. *Mathematical Biosciences & Engineering*, 1(2):361.

[14] Chouinard,D.,Vanoosthuyse,G.,Pelletier,F.,Bellerose,F.,Bourgeois,S.,andDominique, P. (2015). A Phenology Model for Codling Moth Management in Quebec Apple Orchards. *Acta Horticulturae*, 1068(5):51–56.

[15] Gianni, G., Pasquali, S., Parisi, S., and Winter, S. (2014). Modelling the Potential Distribution of Bemisia Tabaciin Europe in Light of the Climate Change scenario. *Pest Management science*, 70:1611–1623.

[16] Goh, B. (1976). Global stability in two species interactions. *Journal of Mathematical Biology*, 3(3):313–318.

[17] Ikemoto, Y., Ishikawa, Y., Miura, T., Asama, H. (2009). A mathematical model for caste differentiation in termite colonies (isoptera) by hormonal and pheromonal regulations. *Sociobiology*, 54(3), 841.

[18] Hofmeyr, J. H., Hofmeyr, M., Lee, M., Kong, H., and Holtzhausen, M. (1998). Assessment of a Cold Treatment for the Disinfestations of Export Citrus from False Codling Moth, Thaumatotibia leucotreta (Lepidoptera: Tortricidae): a Report to the People's Republic of China. *Citrus Research International* http://www. citrusres. com/sites/default/files/documents/FCM% 20cold% 20disinfestation% 20study% 20f or% 20Korea, 201998.

[19] FPEAK (2021). Protocols for the Management of the False Codling Moth (Thaumatotibia Leucotreta) in Roses in Kenya. Kenya Flower Council Technical Committee, Kenya Plant Health Inspectorate Service (KEPHIS), Fresh Produce Exporters Association of Kenya (FPEAK), Kenya Agricultural Livestock Research Organization (KALRO) and the Europe-Africa-Caribbean-Pacific Liaison Committee (COLEACP) in the scope of its NExT Kenya programme. https://fpeak.org/wp-content/uploads/2021/05/FCM-Manual.pdf

[20] La Salle, J. P. (1966). An invariance principle in the theory of stability. Space Flight and Guidance Theory,

[21] Liu, X. and Dai, B. (2018). Threshold dynamics of a delayed predator–prey model with impulse via the basic reproduction number. *Advances in Difference Equations*, 2018(1):454.

[22] May, R. M. and Anderson, R. M. (1978). Regulation and Stability of Host-Parasite Population Interactions: II. Destabilizing Processes. The Journal of Animal Ecology, pages 249–267.

[23] Mkiga, A., Mohamed, S., du Plessis, H., Khamis, F., and Ekesi, S. (2019). Field and Laboratory Performance of False Codling Moth, Thaumatotibia Leucotreta (Lepidoptera: Troticidae) on Orange and Selected Vegetables. *Insects*, 10(3):63.

[24] McCluskey,C. C. (2010) Global stability for an SIR epidemic model with delay and nonlinear incidence. *Nonlinear Analysis: Real World Applications*, 11(4),(2010), 3106-3109

[25] Mondaca, L. L., Da-Costa, N., Protasov, A., Ben-Yehuda, S., Peisahovich, A., Mendel, Z., and Ment, D. (2020). Activity of metarhizium brunneum and beauveria bassiana against early developmental stages of the false codling moth thaumatotibia leucotreta. *Journal of Invertebrate Pathology*, 170:107312.

[26] Murray, J. (2002). Mathematical Biology (eds Antman, SS, Marsden, JE, Sirovich, L. & Wiggins, S.) 175–256. 126

[27] Okongo, M. (2016). Modeling HIV-AIDS Co-Infections with Malaria and Tuberculosis in the Presence of Antiretroviral Treatment and Counseling. PhD thesis, Kenya: Chuka University.

[28] Potgieter, L. (2013a). A mathematical Model for the Control of Eldana Saccharina Walker using the Sterile Insect Technique. PhD thesis, Stellenbosch: Stellenbosch University.

[29] Savary, S., Teng, P. S., Willocquet, L., and Nutter Jr, F. W. (2006). Quantification and Modeling of Crop Losses: *A Review of Purposes. Annu. Rev. Phytopathol*., 44:89– 112.

[30] Sergio, R. (2014). The Optimal Release of Sterile Males in Pest Management. All Graduate Plan B and other Reports, 408. 128

[31] Stibick, J., Bloem, S., Carpenter, J., Ellis, S., and Gilligan, T. (2008). New Pest Pesponse Guidelines: False Codling Moth Thaumatotibia leucotreta. Technical report, USDA– APHIS–PPQ–Emergency and Domestic Programs, Riverdale, Maryland. http . . . .

[32] Ullah, R., Zaman, G., and Islam, S. (2013). Stability analysis of a general sir epidemic model. *VFAST Transactions on Mathematics*, 1(1):57–61.

[33] Van den Driessche, P. and Watmough, J. (2002). Reproduction numbers and sub-threshold endemic equilibria for compartmental models of disease transmission. *Mathematical biosciences*, 180(1-2):29–48.

[34] Venette, R. C., Davis, E. E., DaCosta, M., Heisler, H., and Larson, M. (2003). Mini Risk Assessment False Codling Moth, Thaumatotibia (Cryptophlebia) leucotreta (Meyrick)(Lepidoptera: Tortricidae). University of Minnesota, Department of Entomology, CAPS PRA, pages 1–30.

[35] Verreynne, S. et al. (2009). Fruit size and crop load prediction for citrus. *SA Fruit Journal*, 8(5):63–67.

[36] Witzgall, P., Kirsch, P., and Cork, A. (2010). Sex Pheromones and their Impact on Pest Management. *Journal of Chemical Ecology*, 36(1):80–100.

Vol18,4p1.wordcount.tex